



A Buck & Boost based Grid Connected PV Inverter Maximizing Power Yield from Two PV Arrays in Mismatched Environmental Conditions

Koppiseti. Sai Satya Priya | T.lakshmi Narayana | K Manoz Kumar Reddy

Department of Electrical and Electronics Engineering, Aditya college of engineering, Surampalem, Kakinada, East Godavari(Dt), AP, India.

To Cite this Article

Koppiseti. Sai Satya Priya, T.lakshmi Narayana and K Manoz Kumar Reddy. A Buck & Boost based Grid Connected PV Inverter Maximizing Power Yield from Two PV Arrays in Mismatched Environmental Conditions. International Journal for Modern Trends in Science and Technology 2022, 8(12), pp. 78-85. <https://doi.org/10.46501/IJMTST0812013>

Article Info

Received: 18 November 2022; Accepted: 10 December 2022; Published: 13 December 2022.

ABSTRACT

A single phase grid connected transformerless photo voltaic (PV) inverter which can operate either in buck or in boost mode, and can extract maximum power simultaneously from two serially connected subarrays while each of the subarray is facing different environmental conditions, is presented in this paper. As the inverter can operate in buck as well as in boost mode depending on the requirement, the constraint on the minimum number of serially connected solar PV modules that is required to form a subarray is greatly reduced. As a result, power yield from each of the subarray increases when they are exposed to different environmental conditions. The topological configuration of the inverter and its control strategy are designed so that the high frequency components are not present in the common mode voltage thereby restricting the magnitude of the leakage current associated with the PV arrays within the specified limit. Further, high operating efficiency is achieved throughout its operating range. A detailed analysis of the system leading to the development of its mathematical model is carried out. The viability of the scheme is confirmed by performing detailed simulation studies. A 1.5 kW laboratory prototype is developed, and detailed experimental studies are carried out to corroborate the validity of the scheme.

Keywords : Grid connection, Single phase, Transformerless, Buck & Boost based PV inverter, Maximum power point, mismatched environmental condition, Series connected module.

1. INTRODUCTION

The major concern of a photo voltaic (PV) system is to ensure optimum performance of individual PV modules in a PV array while the modules are exposed to different environmental conditions arising due to difference in insolation level and/or difference in operating temperature. The presence of mismatch in operating condition of modules significantly reduces the power output from the PV array [1]. The problem with the

mismatched environmental conditions (MEC) becomes significant if the number of modules connected in series in a PV array is large. In order to achieve desired magnitude for the input dc link voltage of the inverter of a grid connected transformerless PV system, the requirement of series connected modules becomes high. Therefore, the power output from a grid connected transformerless (GCT) Manuscript received July 12, 2017; revised October 10, 2017; accepted October 31,

2017. S. Dutta and K. Chatterjee are with the Department of Electrical Engineering, Indian Institute of Technology Bombay, Mumbai 400076, India (e-mail: subdut87@gmail.com; kishore@ee.iitb.ac.in). PV system such as single phase GCT (SPGCT) inverter based systems derived from H-bridge [2], [3] and neutral point clamp (NPC) inverter based systems [4], [5] get affected significantly during MEC. In order to address the problem arising out of MEC in a PV system, various solutions are reported in the literature. An exhaustive investigation of such techniques has been presented in [6]. Power extraction during MEC can be increased by choosing proper interconnection between PV modules [6], [7] or by tracking global maximum power point (MPP) of PV array by employing complex MPP tracking (MPPT) algorithm [6], [8]. However, these techniques are not effective for low power SPGCT PV system. Similarly, reconfiguration of the PV modules in a PV array by changing the electrical connection of PV modules [9], [10] is not effective for SPGCT PV system due to the considerable increment in component count and escalation in operating complexity. In order to extract maximum power from each PV module during MEC, attempts have been made to control each PV module in a PV array either by having a power electronic equalizer [11] or by interfacing a dc to dc converter [1], [12]- [14]. Schemes utilizing power electronic equalizer require large component count thereby increasing the cost and operation complexity of the system. The scheme presented in [1] uses generation control circuit (GCC) to operate each PV module at their respective MPP wherein the difference in power between each module is only processed through the GCC. Scheme presented in [12] uses shunt current compensation of each module as well as series voltage compensation of each PV string in a PV array to enhance power yield during MEC. The schemes based on module integrated converter [13], [14] use dedicated dc to dc converter integrated with each PV module. However, the efficiency of the aforesaid schemes are low due to the involvement of large number of converter stages, and further in these schemes the component count is high and hence they face similar limitations as that of power electronic equalizer based scheme. Instead of ensuring MPP operation of each and every module, certain number of modules are connected in series to form a string and the so formed

strings are then made to operate under MPP in [15], [16]. Even then there is not much reduction in overall component count and control complexity [6]. In order to simplify the control configuration and to reduce the component count, schemes reported in [17], [18] combine all the PV modules into two subarrays, and then each of the subarray is made to operate at their respective MPP. However, the reported overall efficiency of both the schemes are poor. By introducing a buck and boost stage in SPGCT PV inverter, power extraction during MEC is improved in [19]- [21]. Further, as a consequence of the presence of the intermediate boost stage, the requirement of series connected PV modules in a PV array has become less. In the schemes presented in [19]- [21], the switches of either the dc to dc converter stage or inverter stage operate at high frequency, as a result there is a considerable reduction in the size of the passive element count, thereby improving the operating efficiency of these schemes. Further, the reported efficiency of [20] and [21] is 1-2 % higher than that of [19]. An effort has been made in this paper to divide the PV modules into two serially connected subarrays and controlling each of the subarray by means of a buck and boost based inverter so that optimum power evacuation from the subarrays is ascertained during MEC. This process of segregation of input PV array into two subarrays reduces the number of series connected modules in a subarray almost by half compared to that of the schemes proposed in [20], [21]. The topological structure and control strategy of the proposed inverter ensure that the magnitude of leakage current associated with the PV arrays remains within the permissible limit. Further, the voltage stress across the active devices is reduced almost by half compared to that of the schemes presented in [20], [21], hence very high frequency operation without increasing the switching loss is ensured. High frequency operation also leads to the reduction in the size of the passive elements. As a result the operating efficiency of the proposed scheme is high. The measured peak efficiency and the European efficiency (η_{euro}) of the proposed scheme is found to be 97.65% and 97.02% respectively. The detailed operation of the proposed inverter with mathematical validation is explained in Section II. Afterwards the mathematical model of the proposed inverter has been derived in Section III followed by the philosophy of control

strategy in Section IV. The criteria to select the values of the output filter components are presented in Section V. The proposed scheme is verified by performing extensive simulation studies and the simulated performance is presented in Section VI. A 1.5 kW laboratory prototype of the proposed inverter has been fabricated to carry out thorough experimental studies. The measured performances of the scheme which confirm its viability are presented in Section VII.

2. PROPOSED INVERTER AND ITS OPERATION

The schematic of the proposed Dual Buck & Boost based Inverter (DBBI) which is depicted in Fig. 1 is comprising of a dc to dc converter stage followed by an inverting stage. The dc to dc converter stage has two dc to dc converter segments, CONV1 and CONV2 to service the two subarrays, P V1 and P V2 of the solar PV array. The segment, CONV1 is consisting of the self-commutated switches, S1 along with its anti-parallel body diode, D1, S3 along with its anti-parallel body diode, D3, the free wheeling diodes, Df1, Df3 and the filter inductors and capacitors, L1, Cf1, and Co1. Similarly, the segment, CONV2 is consisting of the self-commutated switches, S2 along with its anti-parallel body diode, D2, S4 along with its anti-parallel body diode, D4, the free wheeling diodes, Df2, Df4 and the filter inductors and capacitors, L2, Cf2, and Co2. The inverting stage is consisting of the self-commutated switches, S5, S6, S7, S8, and their corresponding body diodes, D5, D6, D7 and D8 respectively. The inverter stage is interfaced with the grid through the filter inductor, Lg. The PV array to the ground parasitic capacitance is modeled by the two capacitors, Cpv1 and Cpv2

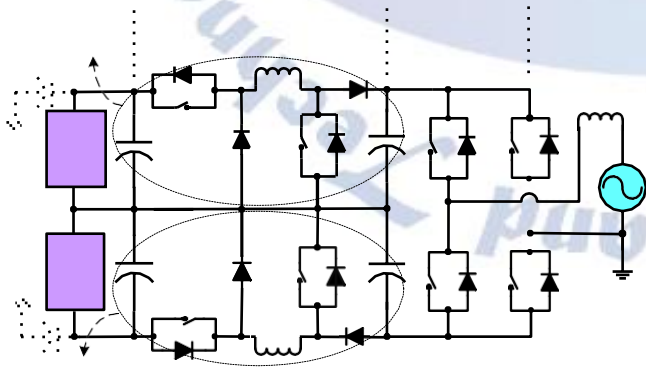


Fig.1. Dual Buck & Boost based Inverter (DBBI)

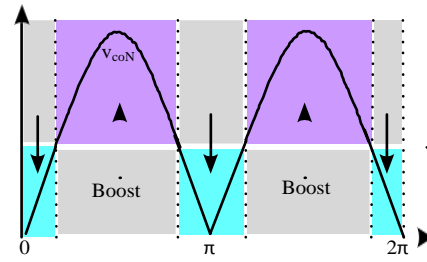
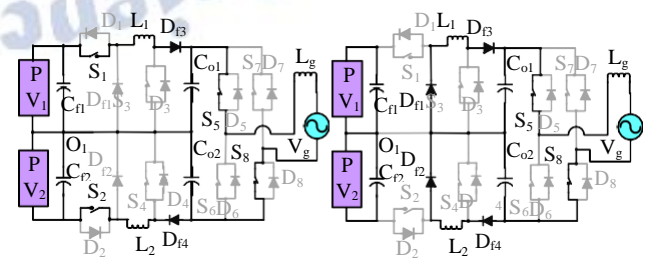


Fig.2. Buck stage and Boost stage of the proposed inverter

Considering Fig. 2, CONV1 operates in buck mode when $V_{pv1} \geq V_{co1}$, while CONV2 operates in buck mode when $V_{pv2} \geq V_{co2}$. V_{pv1} , V_{pv2} are the MPP voltages of PV1 and PV2 and V_{co1} , V_{co2} are the output voltages of CONV1 and CONV2 respectively. During buck mode duty ratios of the switches, S1 and S2 are varied sinusoidally to ensure sinusoidal grid current (i_g) while S3 and S4 are kept off. When $V_{pv1} < V_{co1}$, CONV1 operates in boost mode while CONV2 operates in boost mode when $V_{pv2} < V_{co2}$. During boost mode duty ratios of the switches, S3 and S4 are varied sinusoidally to ensure sinusoidal i_g while S1 and S2 are kept on throughout this mode. The sinusoidal switching pulses of the switches of CONV1 and CONV2 are synchronized with the grid voltage, v_g to accomplish unity power factor operation. The switches, S5 and S8 are kept on and switches S6 and S7 are kept off permanently during the entire positive half cycle (PHC) while during entire negative half cycle (NHC), the switches, S6 and S7 are kept on and switches, S5 and S8 are kept off permanently. All the operating states of the proposed inverter are depicted in Fig. 3.

When the insolation level and ambient temperature of sub-array PV1 are different from that of PV2, the MPP parameters



(a)

(b)

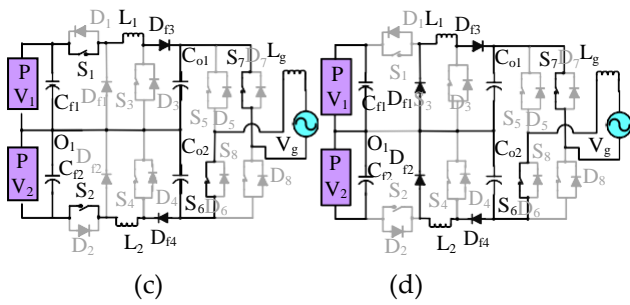


Fig Operating states of DBBI: (a) Active and (b) Freewheeling states in buck mode of PHC, (c) Active and (d) Freewheeling states in buck mode of NHC, (e) Active and (f) Freewheeling states in boost mode of PHC, (g) Active and (h) Freewheeling states in boost mode of NHC

of the two subarrays, V_{pv1} and V_{pv2} , MPP current, I_{pv1} and I_{pv2} correspond to PV_1 and PV_2 respectively and power at MPP, P_{pv1} and P_{pv2} correspond to PV_1 and PV_2 respectively differ from each other. By considering that both the subarrays are operating at their respective MPP and neglecting the losses incurred in power processing stages, the average power involved with C_{o1} and C_{o2} , P_{co1} and P_{co2} over a half cycle can be assumed equal to the power extracted from PV_1 and PV_2 . Therefore,

$$P_{co1} = P_{pv1} \quad \& \quad P_{co2} = P_{pv2} \quad (1)$$

The power injected to the grid averaged over a half cycle, P_g can be written as

$$P_g = P_{pv1} + P_{pv2} \quad (2)$$

Further, at any half cycle

$$v_g = v_{co1} + v_{co2} \quad (3)$$

Hence, the instantaneous injected power to the grid, p_g can be written as

$$p_g = v_g i_g = (v_{co1} + v_{co2}) i_g \quad (4)$$

wherein v_{co1} and v_{co2} denote the instantaneous quantities of V_{co1} and V_{co2} respectively. As i_g is in-phase with v_g ,

$$I_g = P_g / V_g \quad (5)$$

wherein V_g and I_g denote rms values of v_g and i_g respectively. The power injected to the grid can be expressed as

$$P_g = 1/\pi \int_0^\pi \pi \cdot 0 \cdot p_g \, d(\omega t) = 1/\pi \int_0^\pi \pi \cdot 0 \cdot v_{co1} i_g \, d(\omega t) + 1/\pi \int_0^\pi \pi \cdot 0 \cdot v_{co2} i_g \, d(\omega t) \quad (6) = P_{co1} + P_{co2} \quad (7)$$

As v_{co1} and v_{co2} are synchronized with v_g . Hence $P_{co1} = 1/\pi \int_0^\pi \pi \cdot 0 \cdot V_{co1m} \sin(\omega t) I_{gm} \sin(\omega t) \, d(\omega t) = V_{co1m} I_{gm} / 2 \quad (8)$

$$\text{Similarly, } P_{co2} = V_{co2m} I_{gm} / 2 \quad (9)$$

wherein the amplitudes of v_{co1} , v_{co2} and i_g are denoted as V_{co1m} , V_{co2m} and I_{gm} respectively. Combining (1), (8) and (9)

$$V_{co1m} = 2 P_{pv1} / I_{gm} = \sqrt{2 P_{pv1}} I_g = \sqrt{2 P_{pv1}} P_g / V_g \quad (10)$$

$$V_{co2m} = 2 P_{pv2} / I_{gm} = \sqrt{2 P_{pv2}} I_g = \sqrt{2 P_{pv2}} P_g / V_g \quad (11)$$

Similarly by combining (2), (10) and (11),

$$V_{co1m} = V_m P_{pv1} / (P_{pv1} + P_{pv2}) \quad \& \quad V_{co2m} = V_m P_{pv2} / (P_{pv1} + P_{pv2}) \quad (12)$$

The voltage templates of v_{co1} and v_{co2} appear as full wave rectified sinusoidal waveform with amplitudes, V_{co1m} and V_{co2m} respectively. V_m is the amplitude of v_g . It can be deduced from (12) that the magnitudes of V_{co1m} and V_{co2m} are decided by the power extracted from each of the subarray. If the power extracted from PV_1 is less than PV_2 , then $V_{co1m} < V_{co2m}$, whereas $V_{co2m} < V_{co1m}$ if power extracted from PV_2 is less than PV_1 . During buck mode, the duty ratios, d_1 of S_1 and d_2 of S_2 vary sinusoidally with an amplitude d_{1m} and d_{2m} ,

$$\text{wherein } d_{1m} = V_{co1m} / V_{pv1} \quad \& \quad d_{2m} = V_{co2m} / V_{pv2} \quad (13) \text{ while during boost mode the duty ratios, } d_3 \text{ of } S_3 \text{ and } d_4 \text{ of } S_4 \text{ vary sinusoidally with amplitude } d_{3m} \text{ and } d_{4m},$$

$$\text{wherein } d_{3m} = 1 - V_{pv1} / V_{co1m} \quad \& \quad d_{4m} = 1 - V_{pv2} / V_{co2m} \quad (14)$$

The CONV1 and CONV2 are having the same output current i_g . Hence, the input side currents before getting filtered by input filter capacitors of CONV1, i_{sw1} and CONV2, i_{sw2} can be related with i_g in the buck mode by considering the switching cycle average of corresponding quantities as follows i_{sw}

$$i_{1Ts} = d_1 i_{Ts} + (1 - d_1) i_g \quad (15)$$

$$i_{2Ts} = d_2 i_{Ts} + (1 - d_2) i_g \quad (16)$$

Similarly, by considering switching cycle average of corresponding quantities the relation between i_{sw1} ,

isw2 and ig can be deduced during boost mode as

$$\text{hisw1iTs} = h_1 i_1 - d_3 i_3 \text{Ts} \text{higiTs} \quad (17)$$

$$\text{hisw2iTs} = h_1 i_1 - d_4 i_4 \text{Ts} \text{higiTs} \quad (18)$$

Therefore, it can be inferred from (12) and (13) that if the insolation level of P V1 is lower than that of P V2, during buck mode, $d_{1m} < d_{2m}$, thereby $hd_{1iTs} < hd_{2iTs}$ whereas during boost mode as per (12) and (14), $d_{3m} < d_{4m}$, thereby $hd_{3iTs} < hd_{4iTs}$. Hence, it can be concluded from (15), (16), (17) and (18) that in any operating mode, $\text{hisw1iTs} < \text{hisw2iTs}$, therefore $I_{pv1} < I_{pv2}$. Following the same argument, $I_{pv1} > I_{pv2}$ if the insolation level of P V1 is higher than that of P V2. Considering Fig. 1 it can be noted that during operation in PHC, $v_{cpv1} = v_{co2} + V_{pv1}$, $v_{cpv2} = v_{co2} - V_{pv2}$ while during NHC $v_{cpv1} = v_{co1} + V_{pv1}$, $v_{cpv2} = v_{co1} - V_{pv2}$, wherein v_{cpv1} and v_{cpv2} are the voltages impressed across C_{pv1} and C_{pv2} respectively. Hence, the voltages across C_{pv1} and C_{pv2} contains insignificant amount of dc and low frequency components which also ensures that the magnitude of the leakage current is maintained within the limit specified in the standard, VDE0126-1-1, and also cited in [23].

3. CONTROL STRATEGY OF THE PROPOSED SCHEME

The control strategy of the proposed scheme is depicted in Fig. 5. The controller is designed to fulfill the following objectives: i) both subarrays operate at their corresponding MPP simultaneously, ii) sensing of output voltages, v_{co1} and v_{co2} are not required, iii) i_g is sinusoidal and is in-phase with v_g throughout the operating range. Two separate MPP trackers and two proportional integral (PI) controllers are employed to determine the value of P_{pv1} and P_{pv2} which are required to estimate V_{co1m} and V_{co2m} . Using (12), V_{co1m} and V_{co2m} are determined where the information of V_m is obtained from the phase locked loop (PLL). A rectified version of a unity sinusoidal function, R is generated from a unity sinusoidal function, X , synchronized with v_g , and is obtained from the same PLL. R is multiplied with V_{co1m} and V_{co2m} to estimate v_{co1} and v_{co2} . Hence, two voltage sensors which otherwise would have been required to determine v_{co1} and v_{co2} get eliminated. V_{pv1} and v_{co1} are compared to decide about the mode of operation

(buck mode or boost mode) of CONV1, while V_{pv2} and v_{co2} are compared to determine the mode of operation of CONV2. RMS values of v_{co1} and v_{co2} are estimated which are then subsequently squared and are then divided by P_{pv1} and P_{pv2} to obtain the emulated effective resistances, R_{pco1} and R_{pco2} of the two component converters. Subsequently the reference current, i_{L1ref} of L1 and the reference current, i_{L2ref} of L2, are synthesized by utilizing (28) in the buck mode [21],

$$i_{L1ref} = v_{co1} R_{pco1} \text{ and } i_{L2ref} = v_{co2} R_{pco2} \quad (28)$$

while for boost mode (29) is used to generate i_{L1ref} and i_{L2ref} [21].

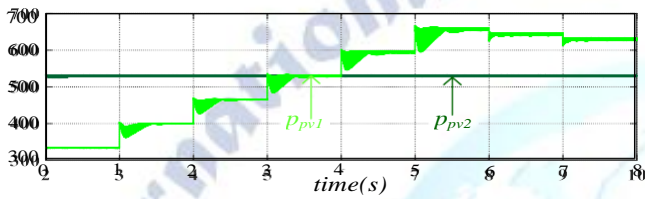
$$i_{L1ref} = v_{co1} R_{pco1} V_{pv1} \text{ and } i_{L2ref} = v_{co2} R_{pco2} V_{pv2} \quad (29)$$

The sensed inductor currents, i_{L1} and i_{L2} are compared with their corresponding references i_{L1ref} and i_{L2ref} . The errors so obtained are processed through two separate PI controllers to generate the required sinusoidal duty ratios for the switches, S1 and S2 during buck mode. Similarly, two separate PI controllers are engaged to process the generated errors to synthesize required sinusoidal duty ratios for switches S3 and S4 during boost mode. Signal Y is used to generate gating signals for S5, S8 while signal Z is used to generate gating signals for S6, S7 of the grid frequency unfolding inverter.

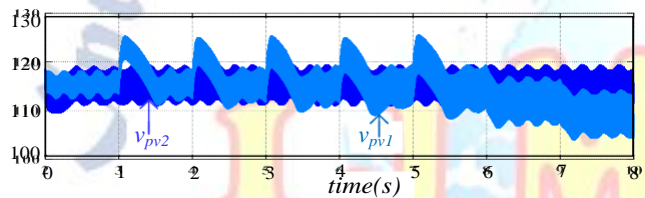
4. SIMULATION STUDY

To demonstrate the efficacy of the proposed inverter a PV array consisting of two PV subarrays while each of the subarray having four series connected Canadian solar polycrystalline modules 'CS6P-165PE' [25] is considered. The MPP parameters of each subarray at standard test condition (STC) are as follows: $V_{pv1} = V_{pv2} = 116$ V, $I_{pv1} = I_{pv2} = 5.7$ A and $P_{pv1} = P_{pv2} = 661$ W. The parameters which are used to simulate the proposed inverter are indicated in Table I. MATLAB Simulink platform is utilized to simulate the performance of the proposed inverter. The variation in insolation level and temperature with respect to time which is considered for the two subarrays to demonstrate the effectiveness of the proposed inverter are tabulated in Table II. Estimated variation of P_{pv1} , P_{pv2} along with the other parameters I_{gm} , V_{co1m} , V_{co2m} , peak of i_{L1} (I_{L1m}) and peak of i_{L2} (I_{L2m}) are also indicated in the same table. Fig. 6(a)-(c) represents

the variation of P_{pv1} , P_{pv2} , V_{pv1} , V_{pv2} , I_{pv1} , I_{pv2} of the two subarrays and also demonstrate the ability of the proposed inverter to operate the two subarrays simultaneously at their respective MPP. Variation in i_g , i_{L1} , i_{L2} , v_{co1} and v_{co2} along with their magnified versions for two different insolation levels are depicted in Figs. 7 to 9. The estimated values of the aforementioned quantities as tabulated in Table II conform to that of obtained through simulation studies thereby ensuring the viability of the proposed scheme.



(a)



(b)

Simulated waveform: Variation in (a) p_{pv1} and p_{pv2} , (b) v_{pv1} and v_{pv2}

5. EXPERIMENTAL VERIFICATION

A 1.5 kW laboratory prototype of the proposed inverter is fabricated and detailed experimental studies have been carried out to demonstrate the effectiveness of the proposed scheme. The photograph of the experimental prototype is shown in Fig. 10. Buck stage Boost stage Inverting stage Sensing board Buffer circuit Driver Fig. 10. Experimental prototype of the proposed inverter The EPS PSI9306-15 power supply has the provision to change only the effect of insolation level while the option to change the effect of temperature is unavailable. In order to emulate simultaneous variation in temperature and level of insolation, the MPP parameters of the two solar emulators (solar emulator 1 as P V1 and solar emulator 2 as P V2) are set as follows at STC: $V_{pv1} = 130$ V, $I_{pv1} = 5$ A and $V_{pv2} = 120$ V, $I_{pv2} = 5$ A. The variation in insolation level of P V1 is indicated in Table III while the insolation level of P V2 is maintained at 80%. The expected values of I_{pv1} , I_{pv2} ,

P_{pv1} , P_{pv2} , V_{co1m} , V_{co2m} , I_{gm} , I_{L1m} , I_{L2m} for the entire operating range are tabulated in the Table III. Fig. 11 depicts the change in i_g , I_{pv1} , I_{pv2} , P_{pv1} , P_{pv2} throughout the range of variation in the level of insolation as specified in Table III. Magnified version of the responses of v_{co1} , v_{co2} , i_{L1} and i_{L2} along with v_g , i_g are also shown in Fig. 12(a) to (f) for two different insolation levels of P V1. The figures Fig. 12(a) and (b) ensure that i_g remains to be sinusoidal and in-phase with v_g in spite of having difference in the magnitude of power being extracted from the two subarrays. From Fig. 12(c) it can be inferred that the converter associated with P V1 operates completely in buck mode, whereas the converter associated with P V2 operates in both buck and boost mode depending on the requirement. Thus, it can be inferred that the two converter segments are able to operate in a decoupled fashion. The measured variables, I_{pv1} , I_{pv2} , P_{pv1} , P_{pv2} , V_{co1m} , V_{co2m} , I_{gm} , I_{L1m} , I_{L2m} as depicted in Figs. 11, 12 are more or less same as that of the estimated ones presented in Table III, and this validates the ability of the proposed inverter to extract maximum power from twosubarrays operating under MEC.

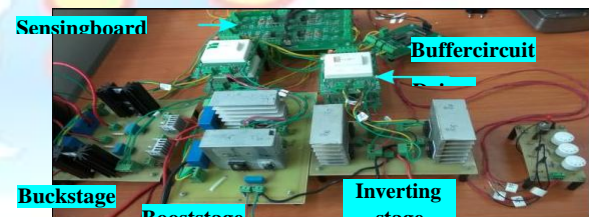


Fig Experimental prototype of the proposed inverter

Fig Shows depicts the Fast Fourier Transform (FFT) of i_g . The THD of i_g is found to be 4.61% which is below the limit of 5% as specified in the standards, IEEE 1574/IEC 61727 [22]. It may be noted that the measured THD of v_g is found to be 2.12% and hence the contribution to THD from the inverter is much less than 4.61%.

The measured and estimated efficiency curves of the proposed inverter are shown Fig. 14. In order to measure the efficiency of the proposed inverter the Yokogawa make power analyzer, WT1800 is used and further, the losses incurred in the active and passive elements of the power circuit is considered while the losses involved with the control circuit are neglected. The efficiency is determined while both V_{pv1} and V_{pv2} are set at 130 V. Measured peak efficiency is found to be

97.65% and the measured European efficiency (η_{euro}) is obtained as 97.02%.

6. CONCLUSION

A single phase grid connected transformerless buck and boost based PV inverter which can operate two subarrays at their respective MPP was proposed in this paper. The attractive features of this inverter were i) effect of mismatched environmental conditions on the PV array could be dealt with in an effective way, ii) operating efficiency achieved, $\eta_{\text{euro}} = 97.02\%$ was high, iii) decoupled control of component converters was possible, iv) simple MPPT algorithm was employed to ensure MPP operation for the component converters, v) leakage current associated with the PV arrays was within the limit mentioned in VDE 0126-1-1. Mathematical analysis of the proposed inverter leading to the development of its small signal model was carried out. The criterion to select the values of the output filter components was presented. The scheme was validated by carrying out detailed simulation studies and subsequently the viability of the scheme was ascertained by carrying out thorough experimental studies on a 1.5 kW prototype of the inverter fabricated for the purpose

Conflict of interest statement

Authors declare that they do not have any conflict of interest.

REFERENCES

- [1] T. Shimizu, O. Hashimoto, and G. Kimura, "A novel high-performance utility-interactive photovoltaic inverter system," *IEEE Trans. Power Electron.*, vol. 18, no. 2, pp. 704-711, Mar. 2003.
- [2] S. V. Araujo, P. Zacharias, and R. Mallwitz, "Highly efficient singlephase transformerless inverters for grid-connected photovoltaic systems," *IEEE Trans. Ind. Electron.*, vol. 57, no. 9, pp. 3118-3128, Sep. 2010.
- [3] B. Ji, J. Wang, and J. Zhao, "High-efficiency single-phase transformerless PV H6 inverter with hybrid modulation method," *IEEE Trans. Ind. Electron.*, vol. 60, no. 5, pp. 2104-2115, May 2013.
- [4] R. Gonzalez, E. Gubia, J. Lopez, and L. Marroyo, "Transformerless single phase multilevel-based photovoltaic inverter," *IEEE Trans. Ind. Electron.*, vol. 55, no. 7, pp. 2694-2702, Jul. 2008.
- [5] H. Xiao and S. Xie, "Transformerless split-inductor neutral point clamped three-level PV grid-connected inverter," *IEEE Trans. Power Electron.*, vol. 27, no. 4, pp. 1799-1808, Apr. 2012.
- [6] A. Bidram, A. Davoudi, and R. S. Balog, "Control and circuit techniques to mitigate partial shading effects in photo voltaic arrays," *IEEE J. Photovolt.*, vol. 2, no. 4, pp. 532-546, Oct. 2012.
- [7] N. D. Kaushika, and N. K. Gautam, "Energy yield simulations of interconnected solar PV arrays," *IEEE Trans. Energy Convers.*, vol. 18, no. 1, pp. 127-134, Mar. 2003.
- [8] H. Patel, and V. Agarwal, "Maximum power point tracking scheme for PV systems operating under partially shaded conditions," *IEEE Trans. Ind. Electron.*, vol. 55, no. 4, pp. 1689-1698, Apr. 2008.
- [9] D. Nguyen, and B. Lehman, "An adaptive solar photovoltaic array using model-based reconfiguration algorithm," *IEEE Trans. Ind. Electron.*, vol. 55, no. 7, pp. 2644-2654, Jul. 2008.
- [10] G. V.-Quesada, F. G.-Gispert, R. P.-Lopez, M. R.-Lumbreras, and A. C.- Roca, "Electrical PV array reconfiguration strategy for energy extraction improvement in grid-connected PV systems," *IEEE Trans. Ind. Electron.*, vol. 56, no. 11, pp. 4319-4331, Nov. 2009.
- [11] L. F. L. Villa, T.-P. Ho, J.-C. Crebier, and B. Raison, "A power electronics equalizer application for partially shaded photovoltaic modules," *IEEE Trans. Ind. Electron.*, vol. 60, no. 3, pp. 1179-1190, Mar. 2013.
- [12] P. Sharma, and V. Agarwal, "Maximum power extraction from a partially shaded PV array using shunt-series compensation," *IEEE J. Photovolt.*, vol. 4, no. 4, pp. 1128-1137, Jul. 2014.
- [13] N. Femia, G. Lisi, G. Petrone, G. Spagnuolo, and M. Vitelli, "Distributed maximum power point tracking of photovoltaic arrays: novel approach and system analysis," *IEEE Trans. Ind. Electron.*, vol. 55, no. 7, pp. 2610-2621, Jul. 2008.
- [14] C. Olalla, C. Deline, D. Clement, Y. Levron, M. Rodriguez, and D. Maksimovic, "Performance of power-limited differential power processing architectures in mismatched PV systems," *IEEE Trans. Power Electron.*, vol. 30, no. 2, pp. 618-630, Feb. 2015.
- [15] E. Karatepe, T. Hiyama, M. Boztepe, and M. C. Olak, "Voltage based power compensation system for photo voltaic generation system under partially shaded insolation conditions," *Energy Convers. and Manage.*, vol. 49, pp. 2307-2316, Aug. 2008.
- [16] A. A. Elserougi, M. S. Diab, A. M. Massoud, A. S. Abdel-Khalik, and S. Ahmed, "A switched PV approach for extracted maximum power enhancement of PV arrays

- during partial shading," *IEEE Trans. Sustain. Energy*, vol. 6, no. 3, pp. 767-772, Jul. 2015.
- [17] I. Patrao, G. Garcera, E. Figueres, and R. Gonzalez-Medina, "Grid-tie inverter topology with maximum power extraction from two photovoltaic arrays," *IET Renewable Power Gener.*, vol. 8, no. 6, pp. 638-648, 2014.
- [18] D. Debnath and K. Chatterjee, "Maximising power yield in a transformerless single phase grid connected inverter servicing two separate photovoltaic panels," *IET Renewable Power Gener.*, vol. 10, no. 8, pp. 1087-1095, 2016.
- [19] N. A. Ahmed, H. W. Lee, and M. Nakaoka, "Dual-mode time-sharing sine wave-modulation soft switching boost full-bridge one-stage power conditioner without electrolytic capacitor DC link," *IEEE Trans. Ind. Appl.*, vol. 43, no. 3, pp. 805-813, May/Jun. 2007.
- [20] Z. Zhao, M. Xu, Q. Chen, J. S. Lai, and Y. Cho, "Derivation, analysis, and implementation of a Boost-Buck converter-based high-efficiency PV inverter," *IEEE Trans. Power Electron.*, vol. 27, no. 3, pp. 1304-1313, Mar. 2012.
- [21] W. Wu, J. Ji, and F. Blaabjerg, "Aalborg inverter a new type of buck in buck, boost in boost grid-tied inverter," *IEEE Trans. Power Electron.*, vol. 30, no. 9, pp. 4784-4793, Sept. 2015.
- [22] R. Teodorescu, M. Liserre and P. Rodriguez, *Grid converters for photovoltaic and wind power systems*, John Wiley & Sons Ltd., 2011, ISBN: 978-0-470-05751-3.
- [23] W. Li, Y. Gu, H. Luo, W. Cui, X. He, and C. Xia, "Topology review and derivation methodology of single phase transformerless photovoltaic inverters for leakage current suppression," *IEEE Trans. Ind. Electron.*, vol. 62, no. 7, pp. 4537-4551, Jul. 2015.
- [24] W. Wu, Y. He, and F. Blaabjerg, "An LLCL power filter for singlephase grid-tied inverter," *IEEE Trans. Power Electron.*, vol. 27, no. 2, pp. 782-789, Feb. 2012.
- [25] Information on Canadian solar module CS6P-165PE. [Online]. Available: www.solarhub.com/product-catalog/pv-modules/124